Cell

Tryptophan Biosynthesis Protects Mycobacteria from CD4 T-Cell-Mediated Killing

Yanjia J. Zhang,[1] Manchi C. Reddy,[2] Thomas R. Ioerger,[3] Alissa C. Rothchild,[4] Veronique Dartois,[5] Brian M. Schuster,[1] Andrej Trauner,[1] Deeann Wallis,[2] Stacy Galaviz,[2] Curtis Huttenhower,[6] James C. Sacchettini,[2] Samuel M. Behar,[4] and Eric J. Rubin[1,*]

[1]Department of Immunology and Infectious Disease, Harvard School of Public Health, Boston, MA 02115, USA
[2]Department of Biochemistry and Biophysics, Texas A&M University, College Station, TX 77842, USA
[3]Department of Computer Science, Texas A&M University, College Station, TX 77842, USA
[4]Department of Microbiology and Physiological Systems, University of Massachusetts Medical School, Worcester, MA 01655, USA
[5]Public Health Research Institute, New Jersey Medical School, Newark, NJ 07103, USA
[6]Department of Biostatistics, Harvard School of Public Health, Boston, MA 02115, USA
*Correspondence: erubin@hsph.harvard.edu
http://dx.doi.org/10.1016/j.cell.2013.10.045

SUMMARY

Bacteria that cause disease rely on their ability to counteract and overcome host defenses. Here, we present a genome-scale study of *Mycobacterium tuberculosis* (Mtb) that uncovers the bacterial determinants of surviving host immunity, sets of genes we term "counteractomes." Through this analysis, we found that CD4 T cells attempt to contain Mtb growth by starving it of tryptophan—a mechanism that successfully limits infections by *Chlamydia* and *Leishmania*, natural tryptophan auxotrophs. Mtb, however, can synthesize tryptophan under stress conditions, and thus, starvation fails as an Mtb-killing mechanism. We then identify a small-molecule inhibitor of Mtb tryptophan synthesis, which converts Mtb into a tryptophan auxotroph and restores the efficacy of a failed host defense. Together, our findings demonstrate that the Mtb immune counteractomes serve as probes of host immunity, uncovering immune-mediated stresses that can be leveraged for therapeutic discovery.

INTRODUCTION

Mycobacterium tuberculosis (Mtb), the etiologic agent of tuberculosis (TB), remains one of the world's major bacterial pathogens. After a century-long decline, the last few decades have seen a resurgence in TB, with an estimated 2 billion people infected and about 1.7 million deaths per year (WHO, 2011). The success of Mtb as a pathogen lies in its adaptation to the human host and its capacity to counteract the many arms of antibacterial immunity (Ernst, 2012). Its ability to survive host defenses is directly responsible for the large reservoir of infected people, whereas its ability to subvert bactericidal mechanisms allows it to replicate in vivo and cause disease (Ehrt and Schnappinger, 2009). Elucidating these mechanisms will help us to understand the complex host-pathogen interface, and targeting these mechanisms is an underutilized therapeutic strategy that can help patients' immune systems kill Mtb.

In the multifaceted immune response against Mtb, CD4 T cells make up one of the most biologically and epidemiologically important compartments. Humans and mice generally cannot clear Mtb during infection, but both are able to limit bacterial growth, and in the case of immunocompetent humans, prevent disease (Ernst, 2012; Flynn, 2006). This response is dependent on CD4 T cells. The CD4-deficient MHC class II knockout (KO) mice, and other mice that lack CD4 T cells, cannot stop mycobacterial growth and rapidly succumb to disease and death (Cosgrove et al., 1991; Grusby et al., 1991; Mogues et al., 2001; Scanga et al., 2000). In human disease, progressive CD4 T cell loss due to HIV infection also increases the risk for TB disease and death (Pawlowski et al., 2012; Selwyn et al., 1989).

However, crucial as they are for TB immunity, CD4 T cells ultimately fail to sterilize infection. The surviving bacteria remain latent, with the potential to cause disease in the future (Ernst, 2012; Flynn, 2006). The nature of the environment imposed by CD4 T cells, enough to limit growth but not kill Mtb, is not well studied. Reports have shown that the Th1 subset is especially effective in limiting Mtb growth, and cytokines such as IFN-γ and TNF-α are needed in some, but not all, models of CD4 T cell-mediated defenses (Bold et al., 2011; Flynn et al., 1993, 1995; Gallegos et al., 2011; Nandi and Behar, 2011; Scanga et al., 2000). But the exact nature of CD4-mediated stress—the repertoire of antipathogen effectors induced by CD4 T cells—is poorly understood. Knowing how CD4 T cells attempt to kill Mtb and how Mtb survives could identify Mtb vulnerabilities and aid drug discovery efforts.

Here, we profile the mycobacterial genetic requirements for surviving the CD4 response, the CD4 "counteractome." We compare this with relevant in vitro survival signatures such as acid, oxidative stress, and nutrient starvation, creating

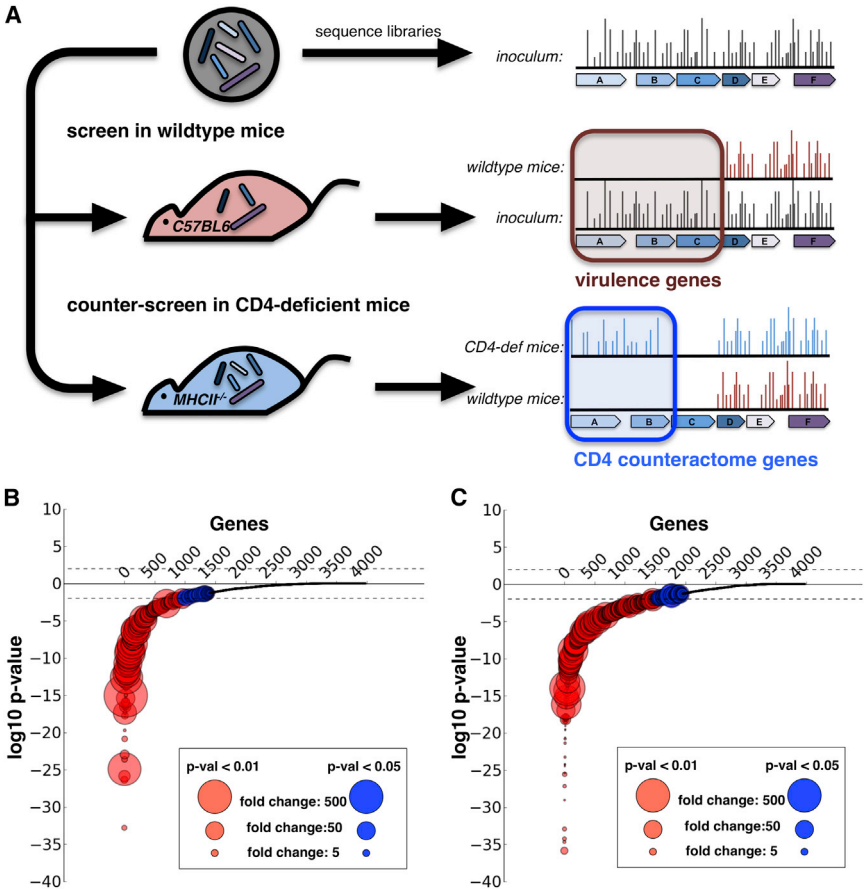

Figure 1. Mtb Genes Required for Infection of WT and *MHCII*$^{-/-}$ Mice

(A) MHC class II KO and WT mice were infected with 10^6 bacilli from our transposon library. At 10 and 45 days after infection, four mice in each group were sacrificed, and spleen homogenates were plated to recover surviving bacteria. To discover genes required for surviving CD4 T cell immunity, we searched for genes that were required for growth in a WT mouse but not required in the MHC class II mice.

(B and C) For both the day 10 (B) and day 45 (C) time points, we calculated for each gene the insertion count differences between the input library and the recovered libraries from WT mice, and a p value expressing the significance of these differences. We then log transformed the p values and gave each gene with a loss of insertions a negative log-p value and each gene with a gain of insertions a positive log-p value. After ordering the genes based on their p values, we plotted each gene as a dot with log-p values on the y axis and the size of the circles representing the fold change of insertion count differences.

See also Figure S1.

counteractomes for physical stresses encountered in the host. Using these, we focus on a particular bacterial pathway, tryptophan (Trp) synthesis, and find the host mechanism for inducing amino acid starvation in intracellular mycobacteria. We go on to find a small molecule that targets Trp synthesis, determine the structural and biochemical basis of its activity, and show that it acts together with the host to kill Mtb both in vitro and during a model infection. Together, our findings demonstrate the utility of profiling the pathogen response to host-mediated stresses. We characterize the stresses induced by CD4 T cells and leverage one stress, Trp starvation, to synergize with a small molecule to more effectively treat TB.

RESULTS

Genes Required for Survival during Infection: Virulence Factors

In order to define the set of Mtb genes required for surviving the CD4 T cell response, we infected both wild-type (WT) and MHC class II KO (*MHCII*$^{-/-}$) mice with a library of Mtb transposon mutants (Zhang et al., 2012). We injected 10^6 bacteria intravenously and plated surviving bacteria from infected spleens at 10 days and 45 days after infection (Figure 1A). To identify mutant Mtb in the surviving pools, we deep sequenced transposon junctions to map the insertion site of each mutant. For each time point, we made two comparisons. First, we compared the surviving pool of mutants from WT mice (WT output library) to the inoculating pool (input library), defining genes with a statistically validated decrease in output library as required for growth during infection, commonly known as virulence factors (Figure 1A). Second, we compared the output library from WT mice to the output library from *MHCII*$^{-/-}$ mice (Figure 1A). In effect, we screened for Mtb mutants with in vivo growth defects that were rescued in the absence of CD4 T cells. We reasoned that genes required for surviving the CD4 T cell response would be required for growth in WT mice, but not required for growth in *MHCII*$^{-/-}$ mice, which lack CD4 T cells (Figure 1A). Because these genes are responsible for counteracting the effects of CD4 T cells, we refer to this set of genes as Mtb's CD4 counteractome.

We found 576 genes that were required for growth during infection (Figures 1B and 1C; see Figure S1A available online). These genes had a statistically significant (false discovery rate [FDR], $q < 0.01$) 10-fold or more decrease in insertion counts across the gene. On day 10, 405 genes were required for growth in vivo, and on day 45, 317 genes were required. A total of 146 genes were required at both time points (Figures 1B and 1C; Table S1). Genes required late but not early could represent mutants that are able to establish infection but unable to sustain long-term in vivo growth. Genes required early but not late could represent mutants that grow slowly in mice. These mutants would be underrepresented at day 10 but catch up by day 45 postinfection. In fact, genes that were required at day 10 but not at day 45 were enriched for loss of insertions (Figure S1B). The average in vitro:in vivo ratio for these genes was 4.3,

compared to the nonrequired average of 1.3 ($p < 0.001$) (Figure S1C). Although this set significantly overlapped with a previously defined set of genes required for growth in mice (gene set enrichment analysis [GSEA], $p < 0.01$), it also includes more than 400 newly discovered genes required for in vivo growth (Figure S2A) (Sassetti and Rubin, 2003).

Genes Required for Surviving CD4-Mediated Stress: The CD4 Counteractome

To screen for the CD4 T cell counteractome, the set of mycobacterial genes required for counteracting CD4-mediated stress, we searched for genes wherein mutations caused a growth defect in WT mice, but not in CD4-deficient mice. By comparing the WT output libraries to the *MHCII*$^{-/-}$ output libraries, we found that 58 genes had a statistically validated increase in insertions in *MHCII*$^{-/-}$ mice compared to WT mice. These genes had at least a 5-fold increase in insertions and a Mann-Whitney U p value of less than 0.05 (Figure 2A; Table S2). Two biochemical pathways, gluconeogenesis and Trp biosynthesis, were enriched in this list, suggesting that CD4 T cells are responsible for inducing a shift in Mtb metabolic demands (Table S2).

The CD4 counteractome could be required for the bacterium's physiologic changes in response to CD4-driven environmental changes. Thus, the counteractome is a signature that cues us into the nature of CD4-mediated stress. To identify these cues, we selected our Mtb transposon library in a series of in vitro models of immune-driven stress conditions and compared the counteractome signatures. Using the same transposon-mapping technique on our selected library, we tested carbon starvation, amino acid starvation (and isolated Trp starvation), iron depletion, acid stress, and nitrosative stress (Tables S3A, S3B, S3C, and S3D). We created conditionally required gene sets as well as ranked gene lists for each condition, which allowed us to compare gene sets using the running-sum enrichment analysis in the GSEA tool (Subramanian et al., 2005). We found that both nitrosative stress and acid stress had significantly similar profiles to genes required for in vivo growth (Figure 2E, pairwise comparisons of "Tyloxapol pH 4.5," "pcit pH 4.5," "DETA-NO," and "in vivo day 45"). This is consistent with the reactive nitrogen species and low pH of Mtb's in vivo niche (Ehrt and Schnappinger, 2009; Vandal et al., 2008). Interestingly, we also found that Trp starvation was enriched in the CD4 counteractome (Figure 2E, intersection of "tryptophan rescue" and "*MHCII*$^{-/-}$ rescue day 9"). Two genes in the Trp biosynthesis pathway, *trpD* and *trpE*, had no insertions in the WT output library but multiple insertions in the *MHCII*$^{-/-}$ output library (Figures 2B and 2C). To confirm this finding, we infected WT and *MHCII*$^{-/-}$ mice with strains of Mtb auxotrophic for Trp. The growth of the auxotrophs was significantly limited in WT mice but restored in *MHCII*$^{-/-}$ mice (Figure 2D). This suggested that CD4 T cells induced the requirement for bacterial Trp biosynthesis and that interfering with Trp metabolism might offer an appealing therapeutic strategy.

Trp Auxotrophy Is Bactericidal

To study the effects of Trp auxotrophy and starvation during Mtb infection, we deleted the *trpE* gene in Mtb and replaced it with a hygromycin-resistance gene (Figure 3A). TrpE, or anthranilate synthase, converts chorismate to anthranilate in the first committed step of Trp biosynthesis. The next enzyme in the pathway, TrpD, converts anthranilate to *N*-(5′-phosphoribosyl)-anthranilate. An Mtb strain carrying a deletion of the *trpD* gene has been shown to be a Trp auxotroph (Figure 3B) (Parish, 2003; Smith et al., 2001). The *trpE* deletion strain grew normally in liquid media only when supplemented with 1 mM Trp (Figure 3C). Interestingly, lower amounts of Trp delayed entry into the logarithmic phase of growth, but the growth dynamics from that point onward was similar to WT. Genetic complementation with the *trpE* gene restored normal growth in media lacking Trp (Figure 3C).

Auxotrophy in Mtb is not always bactericidal (Parish, 2003). Our results suggested that CD4 T cells help starve Mtb of exogenous Trp, so we sought to test the bactericidal potential of blocking endogenous Trp biosynthesis in the face of this exogenous starvation. To do so, we cultured the auxotroph in Trp to both midlog and stationary phase, continued the culture either in the presence or absence of Trp, and measured bacterial survival. The auxotroph was rapidly killed when starved of Trp, suggesting that Trp biosynthesis is an attractive target for a bactericidal drug (Figures 3D and 3E). Interestingly, the *trpE* deletion strains die far more rapidly than a *trpD* deletion (Parish, 2003). The *trpE* deletion strain has about a 100,000-fold loss of viability at 2 weeks, a level that is reportedly not achieved after 13 weeks of starvation of the *trpD* deletion strain. This may be due to accumulation of intermediary metabolites or the presence of an as yet undescribed alternative Trp synthesis pathway.

Trp Auxotrophs Are Hypersusceptible to Macrophages Activated by CD4 T Cells

During a typical lung infection, Mtb first enters alveolar macrophages, which then form an inflammatory structure known as the granuloma. Upon adaptive immune activation, CD4 T cells enter the granuloma and stimulate the infected macrophages (Ernst, 2012). Our screen results suggested that one of these stimulatory mechanisms imposes a need for bacterial Trp biosynthesis, and we sought to delineate the mechanism by which CD4 T cells exert this need. To do so, we infected thioglycolate-elicited mouse peritoneal macrophages with WT Mtb, the *trpE* deletion strain and the complemented strain. Over a 5-day infection, the WT and complemented strains increased in colony-forming units (cfu) by about 5-fold, whereas the *trpE* deletion strain had no measurable growth, demonstrating that Trp biosynthesis is required for growth even in unstimulated macrophages (Figure 4A).

Our mouse findings predicted that the *trpE* deletion strain would be particularly sensitive to CD4-mediated stress. Indeed, the *trpE* deletion strain was significantly hypersusceptible to the effects of CD4 T cells in coculture with macrophages (Figures 4A and 4B). By adding CD4 T cells harvested from the spleens of Mtb-infected mice, macrophages were able to kill the auxotroph more effectively. Compared to unstimulated macrophages, CD4 T cell-stimulated macrophages decreased growth of WT Mtb by about 50%, whereas CD4 coculture decreased *trpE* deletion strain growth by about 80% (Figure 4B). Additionally, the *trpE* deletion strain was also hypersusceptible to IFN-γ and TNF-α, cytokines secreted upon the arrival of CD4 T cells to an Mtb

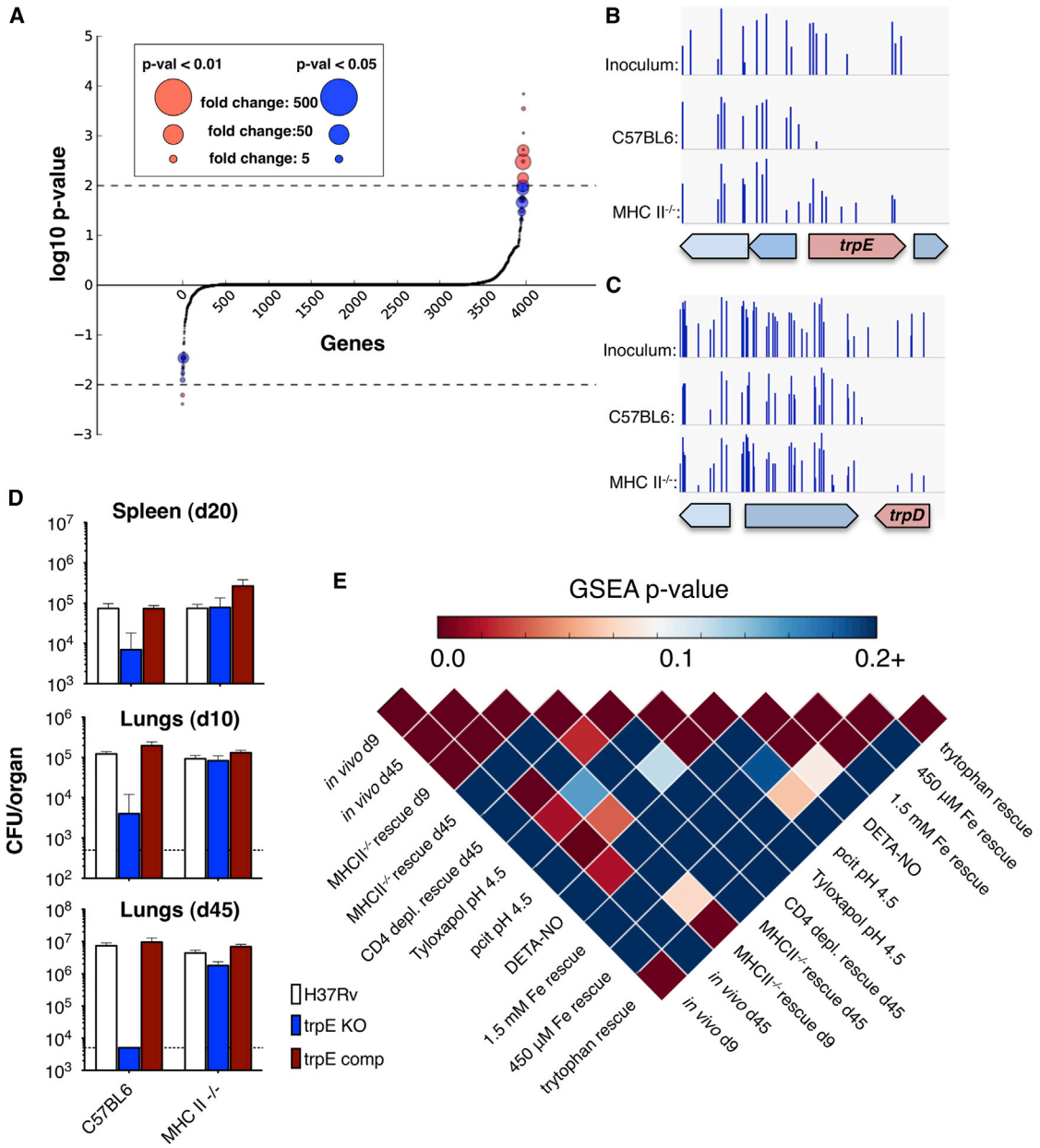

Figure 2. Trp Biosynthesis Is Required during Infection of WT, but Not *MHCII*$^{-/-}$, Mice

(A) To search for genes required for surviving the CD4 T cell response, we identified genes that had a statistically validated increase in insertion counts (above the axis).

(B and C) Transposon insertion counts in the regions containing *trpE* (B) and *trpD* (C) are illustrated. Histograms represent the number of times insertions were found at each potential insertion site. Both *trpE* and *trpD* sustained insertions in our library, but whereas we were unable to retrieve insertions in these genes from WT mice, we were able to recover *trpE* and *trpD* mutants from MHC class II KO mice.

(D) We infected WT, *trpE* KO, and complemented strain Mtb into WT and MHC class II KO mice. Growth of the three strains was determined, confirming the results of our transposon screen. Error bars represent SE.

(E) By comparing gene-requirement signatures, we profiled the similarity of CD4-mediated stress to in vitro models of potential immune-mediated stresses. Each box represents a pairwise comparison between two gene sets, where the larger gene set was ordered by p value and ratio, and the smaller gene set was used by the GSEA preranked tool to search for the enrichment of the second set of genes in the first.

See also Figure S2.

lesion (Figures S3A and S3B). These data confirmed our findings in mice and showed that CD4 T cells and the cytokines they secrete demand the need for mycobacterial Trp biosynthesis during infection. Because human macrophages differ from mouse macrophages in their mycobacterial-killing strategies, we tested the growth of our Mtb strains in monocyte-derived

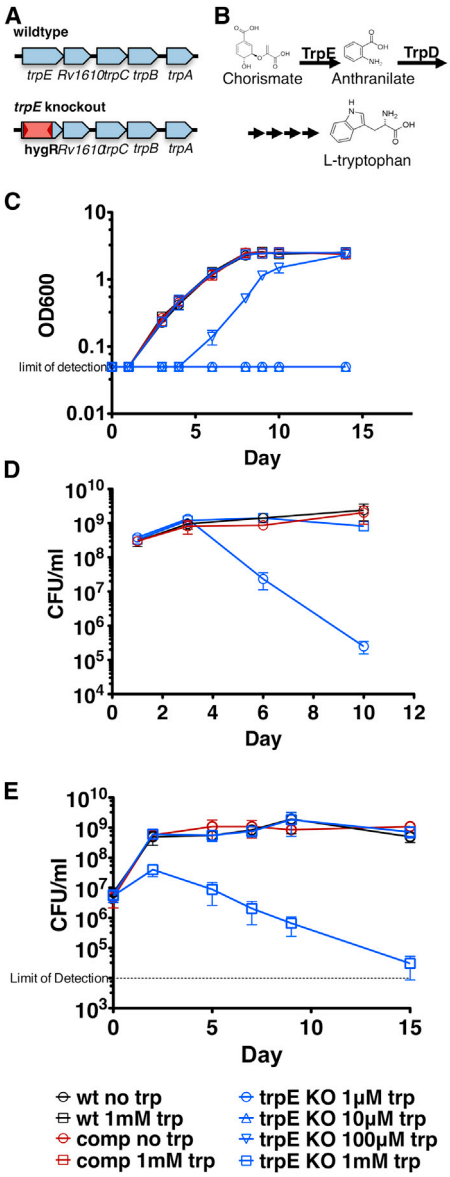

Figure 3. Mtb Trp Auxotrophs Are Cleared during Infection and Die In Vitro during Starvation

(A) We constructed a Trp auxotroph in Mtb by replacing *trpE* with a hygromycin-resistance cassette.

(B) Trp biosynthesis starts with the conversion of chorismate to anthranilate by TrpE, followed by ribosylation by TrpD.

(C) Trp auxotrophs, complemented strains, and WT Mtb were grown in the presence and absence of Trp in 7H9 media. No Trp was required for WT and complement growth, but 1 mM Trp was required to restore normal growth of the Trp auxotroph.

(D and E) Auxotrophs grown to midlog (D) and stationary (E) phase were washed, starved of Trp, and plated for cfu. Starvation of the auxotroph resulted in rapid mycobacterial death.

All error bars denote SEM.

macrophages from human donors. As with previous reports, we observed that IFN-γ alone does not measurably inhibit WT Mtb growth (Fabri et al., 2011). However, whereas the *trpE* deletion strain grew slightly over the 5-day infection, its growth was inhibited by IFN-γ (Figure 4E).

IFN-γ Induction of IDO Necessitates Mycobacterial Trp Biosynthesis

To show that the auxotroph's hypersusceptibility to IFN-γ was Trp dependent, we added Trp to the media in IFN-γ-treated macrophages, which reversed the IFN-γ hypersusceptibility (Figure S3E). As expected, Trp did not change the bacterial growth inhibitory effect of IFN-γ in WT Mtb, showing that Trp supplementation does not have a general growth effect on Mtb (Figure 4E). Interestingly, Trp supplementation could not restore growth of the auxotroph in unstimulated macrophages to WT Mtb levels. It is possible that the levels of Trp needed to restore WT growth (1 mM in liquid broth) cannot be reached intracellularly, whereas the amount of Trp required to protect from IFN-γ-mediated killing could.

Many intracellular pathogens are natural Trp auxotrophs whose intracellular growth is also inhibited by IFN-γ. Thus, we attempted to determine if similar processes affected Trp availability in Mtb infection. One of the transcriptionally induced genes in response to IFN-γ is a Trp-catabolizing enzyme: indoleamine-2,3-dioxygenase (IDO) (Alberati-Giani et al., 1997). IDO utilizes Trp as a synthetic precursor for kynurenines, immune signaling molecules that help control inflammation (Zelante et al., 2009). In this synthetic process, it also greatly decreases the intracellular Trp pool. IDO is thus required for IFN-γ-mediated growth inhibition of *Chlamydia* and other Trp auxotrophic intracellular pathogens (Ibana et al., 2011; Zelante et al., 2009).

We tested the role of IDO in the *trpE* deletion strain's hypersusceptibility to CD4 T cell and IFN-γ by either (1) inhibiting IDO in both human and mouse macrophages with a specific chemical inhibitor, 1-methyl Trp (1-MT) (Figures 4C and 4E), or (2) using mouse macrophages derived from IDO KO mice (Figure 4D). In both cases, the hypersusceptibility was reversed. The inhibitor acts on the macrophage rather than the pathogen because it had no effect on bacteria grown in a defined medium (Figure S3D). These data support that CD4 T cells, likely acting through IFN-γ, stimulate intracellular Trp depletion, forcing Mtb to synthesize its own Trp.

Halogenated Anthranilate Analogs Disrupt Trp Biosynthesis to Kill Mtb In Vitro

Because Trp is required for intracellular growth in the face of CD4-mediated immunity, compounds that inhibit the bacterial Trp synthesis pathway should synergize with host immunity. We focused on anthranilate analogs, compounds that have been shown to inhibit the synthesis of quorum-sensing molecules in *Pseudomonas aeruginosa* that, like Trp synthesis, also have an anthranilate intermediate (Lesic et al., 2007). We tested a panel of anthranilate analogs for Mtb growth inhibition in the presence and absence of Trp. Two fluorinated anthranilates, 2-amino-5-fluorobenzoic acid (5-FABA) and 2-amino-6-fluorobenzoic acid (6-FABA), had an MIC of 5 μM in liquid broth in the absence of Trp (Figure 5A). The addition of Trp blocked toxicity (Figure 5A). 6-FABA was less active against *Mycobacterium smegmatis* (Msm), with an MIC of 65 μM, but this was, again, blocked by added Trp (Figure S4). As predicted from the

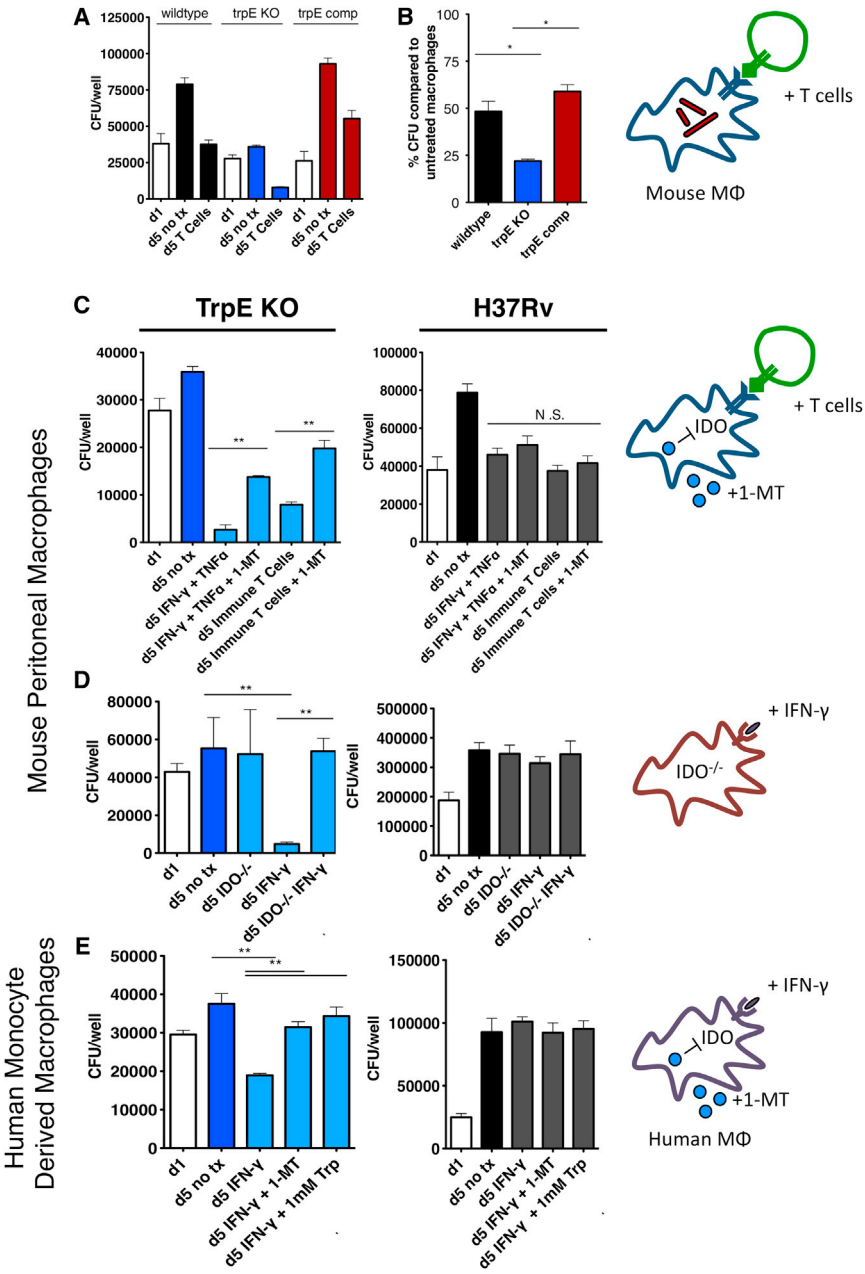

Figure 4. Trp Starvation of Trp Auxotrophs by Macrophages Requires IDO

(A) WT, Trp auxotroph, and complemented strains were used to infect macrophages. One day after infection, macrophages were either stimulated with CD4 T cells in coculture or remained unstimulated.

(B) The Trp auxotroph grew poorly in unstimulated macrophages and was hypersusceptible to the effects of CD4 T cells.

(C) Macrophages were stimulated by either immune CD4 T cells (CD4 T cells isolated from spleens of Mtb-infected mice) or IFN-γ and TNF-α.

(D) To test whether the hypersusceptibility of the auxotroph was dependent on IDO, we also inhibited IDO with its small-molecule inhibitor, 1-MT, or used macrophages isolated from IDO KO mice.

(E) Human monocyte-derived macrophages were infected with WT and Trp auxotroph bacteria. After stimulation with IFN-γ, we showed that the Trp auxotroph was also hypersusceptible to the effects of human IFN-γ.

See also Figure S3.

experiments with auxotrophs, 6-FABA was also bactericidal in liquid broth (Figure 5B) with an ~100-fold and ~10,000-fold decrease in cfu compared to the starting inoculum or the untreated control on day 6, respectively.

To determine the likely target of these compounds, we selected for mutants on solid media containing 150 μM 5-FABA or 300 μM 6-FABA. We plated 10^9 bacteria treated with 0.25% ethyl methanesulfonate on 150 μM 5-FABA, which resulted in ~30 resistant colonies. We then sequenced the genome of a resistant clone and found the following polymorphisms: TrpE:F68I, Rv2585c:A154V, Pks13:P568A, and 4359303:A > G (downstream of RD1 deletion). The *trpE* mutation was surprising because the enzyme converts chorismate into anthranilate, and we had hypothesized that TrpD, which utilizes anthranilate, would be the target of these anthranilate analogs. This led to two competing hypotheses for the mechanism of resistance. The FABA molecules could target TrpE by inhibiting the enzyme at its allosteric site, and the F68I mutation might confer resistance to this targeting. Alternatively, the F68I mutant could be a hypermorph, and insensitivity to allosteric inhibition by Trp might confer resistance through increased Trp synthesis.

Testing the possibility that the FABAs are inhibitors of TrpE activity was technically challenging. We cloned and purified both WT and the F68I mutant form of TrpE and assayed their activity by measuring the fluorescent product, anthranilate (Baker and Crawford, 1966). Both anthranilate-derivative FABA compounds had fluorescent spectra that overlapped with anthranilate. Therefore, we were unable to assess the possibility of the FABA compounds being inhibitors of TrpE. However, we were able to test the enzymatic properties of both mutant and WT TrpE and address the possibility of a hypermorphic allele. Indeed, we found that the mutant enzyme had a 3-fold increase in in vitro activity compared to the WT enzyme (Figure 5C). Furthermore, the mutant enzyme was ~50 times less sensitive to allosteric inhibition by Trp in vitro (Figure 5D). When we modeled the Mtb TrpE structure using the *Serratia marcescens* homolog, we found that F68 resides in the allosteric binding pocket of Trp (Figure 5E). Altogether, this suggests that the F68I mutant is a hypermorphic

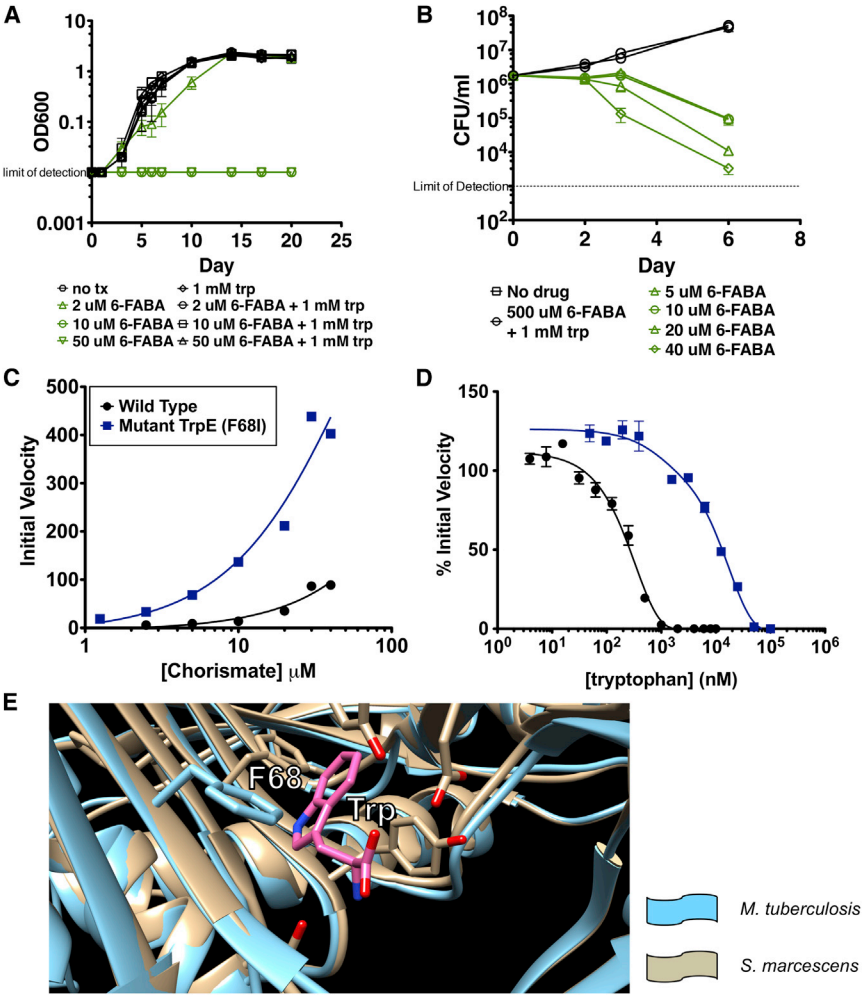

Figure 5. A Small Molecule, 6-FABA, Targets Mycobacterial Trp Biosynthesis

(A) 6-FABA inhibits the growth of Mtb in 7H9. For 6-FABA inhibition of *M. smegmatis* growth, please see Figure S4.

(B) To test the bactericidal potential of 6-FABA, WT Mtb was treated with 6-FABA in 7H9, and cultures were plated for cfu at various time points.

(C) WT (black) and mutant TrpE (F68I; blue) were isolated, and enzymatic activity was assessed by measuring chorismate concentration.

(D) The inhibitory effect of Trp on both WT (blue) and mutant (black) TrpE was measured as percent (%) initial velocity of the no-inhibitor control reaction.

(E) Mtb TrpE structure (blue) was modeled based on the homologous enzyme from *S. marcescens* (beige), showing F68 in the allosteric binding pocket of Trp.

See also Figure S5.

allele that is also less sensitive to allosteric inhibition by Trp. The likely increase in Trp production, then, confers resistance to the FABA compounds in the same way that added exogenous Trp does (Figures 3C–3E).

6-FABA Synergizes with IFN-γ to Kill Mtb in Macrophages

If these compounds act through the Trp biosynthetic pathway, they should phenocopy *trpE* deletion strains during macrophage infection. To test this, we infected macrophages with Mtb and, after 1 day, added 6-FABA and measured bacterial growth by plating for cfu on day 5. At concentrations as low as 10 μM, 6-FABA significantly limited growth by over 10-fold (Figure 6A). The number of cfu at day 5 was lower than at day 1, demonstrating that 6-FABA had bactericidal activity in macrophages. To ensure that activity was not due to the death of macrophages, we tested cytotoxicity and found that 6-FABA did not affect cell viability (Figure S5A).

Because the Trp auxotroph was hypersusceptible to IFN-γ, we hypothesized that 6-FABA's block of Trp biosynthesis would work in synergy with IFN-γ to kill Mtb in macrophages. To test this, we dosed both IFN-γ (10 U/ml) and 6-FABA (0.2 μM) to a level where each individually had about a 2-fold inhibitory effect on bacterial growth (Figure 6B). Without synergy, we predicted that the combined effect of 6-FABA and IFN-γ would be about 4-fold. Instead, the effect was ~40-fold in mouse and ~9-fold in human macrophages, demonstrating clear synergy (Figures 6C, S5B, and S5C).

6-FABA Inhibits Mtb Growth during Infection

Although many compounds are active in vitro, few have adequate bioavailability to be used in animal infections without considerable modification. Fortunately, however, we found that both 6-FABA and an ester derivative (that is rapidly cleaved to the free acid in the circulation) are absorbed orally and achieve high serum concentrations, though with relatively short half-lives (Figure S6). Moreover, doses of up to 250 mg/kg/day did not result in clinical illness or weight loss during a 5-day tolerability trial. This allowed us to test the activity of these compounds in a mouse model of TB.

We infected mice with 10^2 aerosolized Mtb bacilli and allowed infection to establish in the lungs for 8 days. We treated mice six times a week with INH (25 mg/kg/day), 6-FABA (200 mg/kg/day), or the ester derivative (200 mg/kg/day) and planned to measure bacterial growth at 2 and 4 weeks after initiating treatment. Unfortunately, prolonged treatment with 6-FABA resulted in 50% death of animals within 4 weeks. Thus, we could only evaluate 2-week efficacy with this compound. Notably, the ester form of 6-FABA was not toxic, even though it releases the same amount of 6-FABA in mouse serum. This suggested to us that toxicity of 6-FABA was due to an as of yet undetermined off-target effect that might be influenced by an interaction with anesthesia used for gavaging Mtb-infected animals (anesthesia was not used for tolerability trial). Importantly, the nontoxic ester derivative allowed us to assess the in vivo efficacy of pharmaceutical Trp

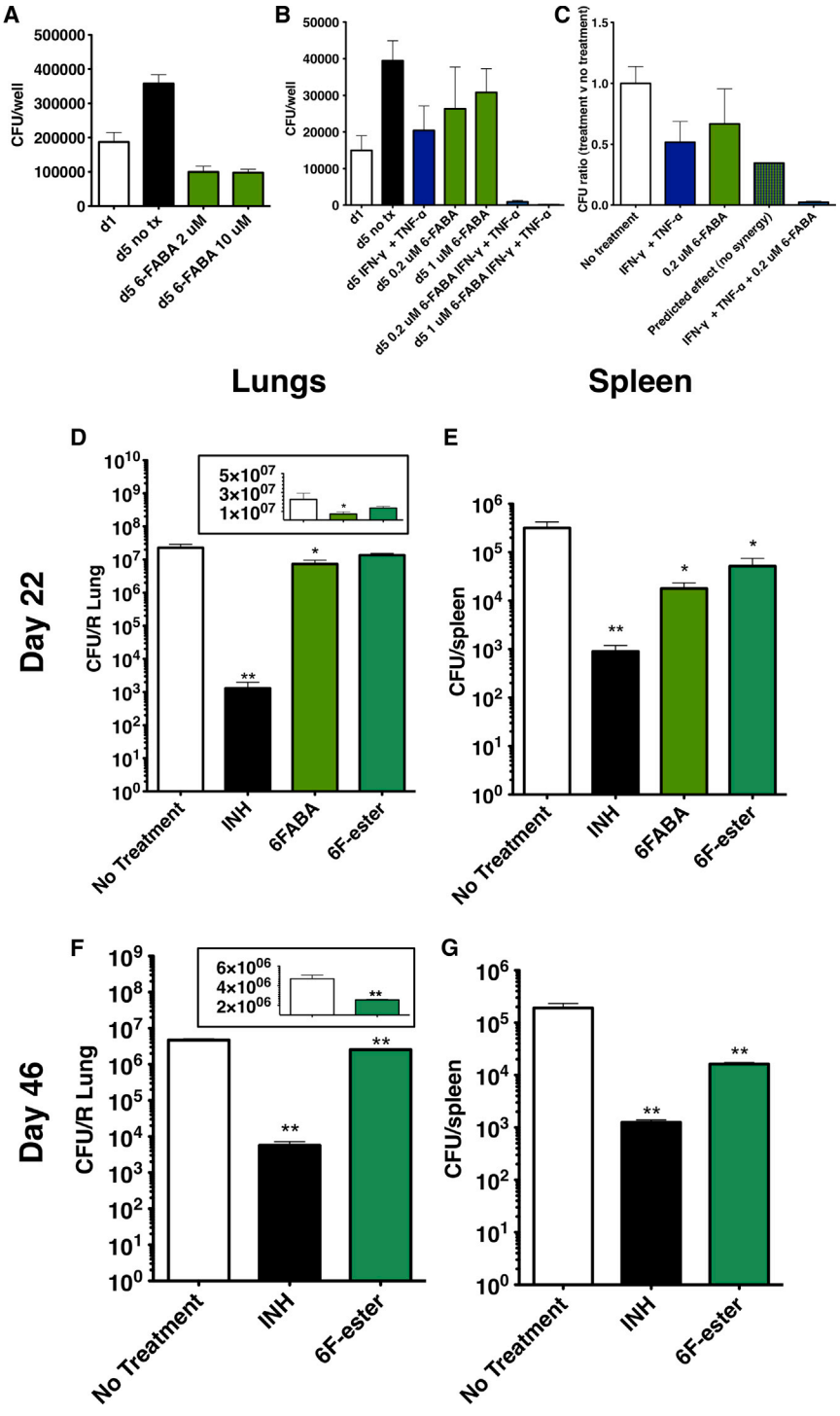

Figure 6. 6-FABA Synergistically Inhibits Mtb Growth in Macrophages and Mice

(A) WT Mtb was used to infect macrophages. On day 1 after infection, macrophages were treated with 6-FABA, and on day 5, cells were lysed and bacteria plated, showing that the 6-FABA was bactericidal in macrophages.

(B) To test the synergy between 6-FABA and IFN-γ, we added 6-FABA and IFN-γ at concentrations that inhibited approximately half of bacterial growth.

(C) Together, their effect was greater than the estimated additive effect of the two molecules in the absence of synergy, showing that they indeed work synergistically to kill Mtb in macrophages. Mice were infected with 10^2 aerosolized Mtb bacilli. After 8 days of infection, mice were treated with INH (25 mg/kg), 6-FABA (200 mg/kg), or with the ester derivative of 6-FABA (200 mg/kg).

(D–G) At 2 weeks (D and E) and 4 weeks (F and G) after infection, lungs and spleens were homogenized and plated for cfu.

*$p < 0.05$ and **$p < 0.01$. Insets show linear scale cfu. Error bars denote SEM.

See also Figure S6.

biosynthesis targeting over a longer time period. At 2 weeks after infection, growth in mouse spleens was decreased by greater than 10-fold in both 6-FABA and the ester derivative-treated mice (Figure 6E). 6-FABA also decreased bacterial growth in the lungs, but to a lesser extent (Figure 6D). At 4 weeks after infection, the ester continued to significantly decrease mycobacterial growth in both spleens and lungs (Figures 6F and 6G). The effect of these molecules on decreasing bacterial growth in vivo demonstrates that Trp biosynthesis is a viable target for drug development. Combined with the fact that CD4 T cells are required for optimal killing of Trp auxotrophs (Figure 2D), we have shown that this therapeutic strategy leverages CD4 T cell activity to kill Mtb in vivo.

DISCUSSION

CD4 T cells are paramount in the host defense against TB but are insufficient to clear the bacteria from a diseased patient. We found that one of the mechanisms by which bacteria survive host CD4-generated stress is through the production of Trp, thus avoiding starvation and death. Loss or inhibition of the Trp biosynthetic pathway renders Mtb hypersusceptible to IFN-γ-mediated killing within macrophages, both in vitro and during infection (Figure 7).

This observation highlights one of the major mechanisms of host protection against invading organisms: depriving them of key nutrients. Infection triggers host responses that sequester important compounds such as amino acids and iron (Hood and Skaar, 2012; Zhang and Rubin, 2013). Although these nonspecific responses are likely important for the control of poorly adapted invaders, successful pathogens have developed strategies to counteract

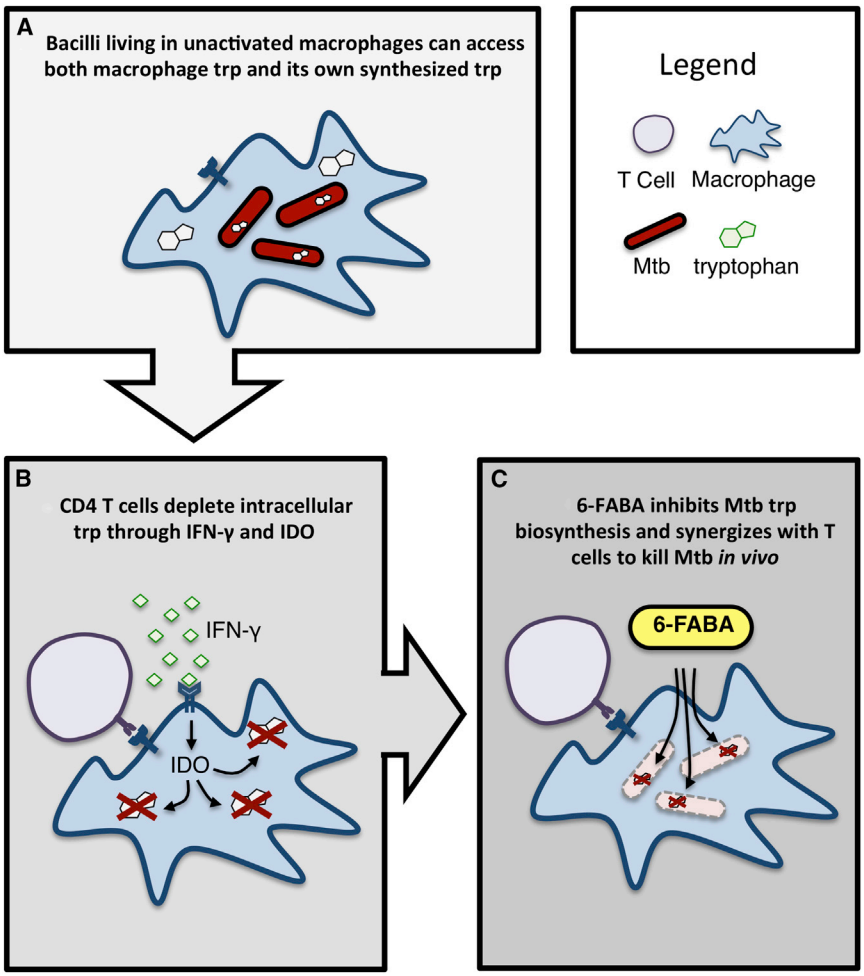

Figure 7. A Model for Trp Starvation as an Antimycobacterial Mechanism

(A) Upon infection, unstimulated macrophages contain high levels of Trp, which together with Trp synthesized by the bacterium is able to support Mtb growth.

(B) CD4 T cells, through IFN-γ and the induction of IDO, decrease the amount of intracellular Trp available to Mtb, demanding the need for mycobacterial Trp biosynthesis for bacterial survival.

(C) Treatment with 6-FABA chemically induces Mtb Trp auxotrophy. Together with immune-mediated Trp starvation, this results in mycobacterial death.

these defenses, including biosynthesis of key compounds and efficient scavenging of others. Mtb in particular relies upon cholesterol and fatty acid catabolism, gluconeogenesis, and the glyoxylate shunt to survive the host environment (Lee et al., 2013; Marrero et al., 2010; McKinney et al., 2000; Muñoz-Elías and McKinney, 2005; Pandey and Sassetti, 2008).

Trp starvation, through IDO-mediated depletion of cytoplasmic pools of this amino acid, appears to be a mechanism that has the added benefit of leading to kynurenine production and prevention of immunopathology (Desvignes and Ernst, 2009). This clearly benefits the host in blocking the growth of cytoplasmic pathogens. However, it is less obvious that it should be a successful strategy for vacuolar organisms that do not have ready access to the cytoplasm. In the case of mycobacteria, susceptibility of Trp auxotrophs to IDO-mediated killing means that bacteria must be able to access this amino acid. This could occur through specific host or bacterial transport mechanisms (that have not been defined) or direct access to the cytoplasm through either partial or complete loss of vacuolar integrity, a model consistent with recent observations of Mtb escape into the cytoplasm (Hagedorn et al., 2009; McDonough et al., 1993; van der Wel et al., 2007). The apparent ability of Mtb to scavenge for Trp points toward a capability to uptake other amino acids. A host of other Mtb amino acid auxotrophs are attenuated for growth in mice; it is possible that this is due to immune-driven starvation mechanisms (Hondalus et al., 2000; Pavelka et al., 2003; Price et al., 2011; Tattoli et al., 2012; Zhang and Rubin, 2013).

Although scavenging Trp in *MHCII*$^{-/-}$ mice allows the Trp deletion strains to survive, it is important to note that these mutants are eventually attenuated even in *MHCII*$^{-/-}$ mice. Similarly, we showed that the *TrpE* deletion strain is attenuated in macrophages even before stimulation by CD4 T cells or IFN-γ and TNF-α. So, whereas our data clearly demonstrate the importance of CD4 T cells in demanding bacterial Trp synthesis, it appears that there may also be CD4-independent mechanisms of Trp starvation. Importantly, this suggests that targeting Trp biosynthesis would retain some effectiveness even in patients, such as HIV-positive individuals, who lack a normal CD4 compartment.

Here, we used an improved analytic approach to identify conditionally essential genes using a transposon library. Each gene has multiple potential insertion sites, and most insertion count comparisons sum counts across each gene to compare between conditions. However, in reasonably saturated libraries, treating each potential insertion site as an independent assessment of gene requirement drastically increased the statistical power of such comparisons. Most transposon insertion-sequencing techniques currently use insertion count totals summed across all sites in a gene (Goodman et al., 2009; Griffin et al., 2011). We found that this drastically decreases the power of statistical hypothesis testing and increases the likelihood that a single differential site could make the entire gene look differentially required. We developed a more discriminating method for assessing the conditional requirement of genes in genome-wide bacterial transposon screens. Using an easily scalable nonparametric test to comprehensively compare the distribution of insertion counts (rather than the sums of insertion counts)

across every gene, we were able to assess genetic requirement across a host of different conditions.

In contrast to similar microarray-based screens, deep sequencing allowed us to directly map insertion sites for each surviving mutant and, thus, improved significantly on the sensitivity and specificity of insertion count comparisons. We found 576 genes that were required for growth in vivo, most of which are newly described as required. Furthermore, by searching for mutants rescued for growth in *MHCII*$^{-/-}$ mice, we described 58 genes that were likely required for surviving CD4-mediated host defenses.

One power of this approach is that we can easily compare gene requirements in multiple conditions, essentially using complex profiles to identify critical environmental determinants. We showed that the in vivo environment as a whole, as well as the specific CD4-generated component of that environment, could be understood by comparing multiple gene-requirement profiles. GSEA comparing in vivo profiles to in vitro profiles confirmed that Mtb's infectious niche is characterized by acidic and oxidative stress and that CD4 T cells impose Trp starvation. Gene-requirement signatures are an effective way to understand both mycobacterial physiology as well as the environments created by components of host immunity. Our study is limited to the determination of the CD4 counteractome, but other counteractomes—those specific to IFN-γ, iNOS, CD8 T cells, or any immune system component that can be perturbed in a mouse—will further our understanding of the tug-of-war between host and pathogen. In fact, given that many CD4-mediated mechanisms are IFN-γ dependent, we would predict that bacterial strains rescued in the *MHCII*$^{-/-}$ mice, like the *trpE* deletion strain, would also be rescued in IFN-γ KO mice. Thus, on a genomics scale, the IFN-γ counteractome should look similar to the CD4 counteractome. Further profiling can test such hypotheses and uncover new mechanistic differences between the many arms of host immunity.

Trp biosynthesis is an attractive target for antibiotic development. Small-molecule inhibitors of Trp and other aromatic amino acid biosynthesis exist for other organisms, suggesting that certain enzymes in these pathways might be "druggable," or suitable for chemical inhibition (Coggins et al., 2003). Furthermore, Trp is an essential amino acid for humans (WHO, 2007) Because hosts get all of their needed Trp from their diets, any cross-species activity of anti-Trp synthesis drugs should be nontoxic (though off-target toxicity remains a possibility).

Halogenated anthranilates were first described as inhibitors of both quorum sensing and growth in *P. aeruginosa* infection (Lesic et al., 2007). We found that two of these compounds, 6-FABA and 5-FABA, had bactericidal activity against Mtb at low concentrations, though only in the absence of Trp. Two lines of evidence suggest that Trp biosynthesis pathway is the physiologic target for both of these compounds. First, normal bacterial growth is restored during FABA treatment by the addition of Trp. Second, resistant mutants harbor a hypermorphic enzyme that is resistant to allosteric inhibition by Trp. Together, these provide chemical and genetic confirmation that Trp can rescue the effect of FABA, but it does not prove that FABA inhibits Trp production. Because TrpD utilizes anthranilate as a substrate, we speculated that 6-FABA might be a competitive inhibitor of TrpD. However, it is also possible that 6-FABA could be a substrate of TrpD, resulting in the production of fluorinated intermediates that inhibit Trp biosynthesis or even fluorinated Trp that incorporates into and poisons protein synthesis or function. Our data clearly demonstrate that the bactericidal activity of 6-FABA is due to its negative effect on Trp biosynthesis, and further studies to elucidate the precise mechanism of toxicity should focus on this Trp effect.

The vast majority of antibiotics are effective against organisms grown in vitro. However, one of the most effective antituberculosis drugs, pyrazinamide, is poorly active under most in vitro growth conditions (Tarshis and Weed, 1953; Zhang and Mitchison, 2003). Instead, it relies on the host environment for efficacy. Similar compounds, which target processes critical in the host, could effectively synergize with the host response to infection and have substantial efficacy. Probing CD4-mediated immunity helped us identify a specific facet of the host-derived environment that could be utilized for bacterial killing. Although we do not yet have a compound that is highly effective during infection, our results provide genetic and chemical validation of the Trp biosynthesis pathway as a target for highly active antibiotics.

EXPERIMENTAL PROCEDURES

Library Generation

Transposon libraries were created as described previously (Zhang et al., 2012) but plated on 7H10 plates with glycerol, OADC, Tween 80, Cas-amino acids, and Trp. A total of 500,000 mutants were scraped, frozen, and saved for future use.

Mouse Infections and Harvests

WT mice (C57BL/6) were obtained from Jackson Laboratory. MHC class II KO mice (Abb H2-Ab1) were obtained from Taconic Farms. Mice were infected with 10^6 bacteria via tail vein injection. At 10 and 45 days postinfection, spleens were harvested and plated for bacteria. For each mouse, 10^6 surviving colonies were scraped, and DNA was extracted for analysis. The protocols, personnel, and animal use were approved and monitored by the Institutional Animal Care and Use Committee. The animal facilities are AAALAC accredited.

In Vitro Transposon Library Selections

For acid stress, the library was suspended in liquid media at a starting concentration of 10^8 cfu/ml and selected in 7H10 with tyloxapol (in place of Tween 80) buffered to pH 6.5 or pH 4.5, and in phosphate-citrate buffer at pH 4.5. Bacteria were plated after 6 days and scraped for DNA prep. For nitrosative stress, the library was suspended in 5 mM DETA-NO for 3 days. Trp starvation and amino acid starvation were measured using libraries that were created either on normal 7H10, or on 7H10 supplemented with 1 mM Trp or 1% Cas-amino acids, respectively. Iron-supplemented libraries were plated on 7H10 with 450 μM and 1.5 mM iron. All primary data can be found in Tables S1, S2, S3, and S4. All the raw data are available in Table S4.

Statistical Analysis

For each insertion count comparison, the control libraries were combined using a script that normalized insertion counts to the sequencing run's total read counts. This combined control library was then used to compare to each experimental library. For each gene, we treated the insertion counts at sites within the middle 90% of the gene as nonparametric distributions and assumed the null hypothesis that the distributions would be the same between conditions. We used a Mann-Whitney U test for hypothesis testing. A p value was thus calculated for each replicate, and a composite p value was generated by using a Bonferroni correction and Fisher's method. We then generated Benjamini-Hochberg FDRs using the composite p values. Ratios were

calculated by averaging the read counts per gene for all replicates and comparing to the combined control library, after normalizing for total read counts.

GSEA

GSEA was performed using the preranked tool. Genes were stratified by p value (<0.01 or 0.05 and > 0.01 or 0.05) and then ranked by ratio within the strata. For each conditional gene-requirement experiment, a ranked list and a conditional essential "calls" gene set were created. Each ranked list was then assessed against each gene set, and familywise error rate was used to generate the p values for significant enrichment.

Construction of *trpE* Deletion and Complement Strains

The hygromycin-resistance gene was amplified with flanks containing 500 bp regions upstream and downstream (and slightly overlapping with) of *trpE*. This construct was electroporated into a recombineering strain of Mtb containing the plasmid pNIT(kan)::RecET-SacB. Transformations were plated on 7H10 agar with 1 mM Trp. Positive clones were plated on 7H10 agar containing 10% sucrose to counterselect against the recombinase plasmid. Deletion of the endogenous locus was confirmed by PCR and by phenotypic tests for auxotrophy. Finally, to complement, the *trpE-rv1610* two-gene operon was amplified and cloned, along with an artificial promoter, using multisite gateway into pDE43-MCK, which integrates into the L5 site.

Macrophage Infections

Peritoneal macrophages were stimulated with thioglycollate medium (3%) by intraperitoneal infection, harvested 3–5 days poststimulation, and isolated using CD11b MicroBeads (Miltenyi Biotec). Human monocyte-derived macrophages were made from donated buffy coats. Ficoll-separated cells were harvested, and macrophages were isolated with CD14 MicroBeads (Miltenyi Biotec) and grown in GM-CSF (10 ng/ml) for 5 days before use. Cells were infected with Mtb at an moi of 10:1 for 2 hr at 37°C and then washed four times. On day 1 postinfection, most conditions were added. To lyse cells, Triton X-100 (0.1%) in PBS was added to each well. Serial dilutions of the lysis were made and plated. For CD4 T cell coculture, we infected mice with 100 aerosolized cfu of Mtb. Spleens from infected mice were harvested no earlier than 6 weeks postinfection, and CD4 T cells were magnetically isolated using a T Cell-Negative Selection Kit (Miltenyi Biotec) and concurrent negative selection of CD8 T cells.

Kinetic Analysis of WT and Mutant Anthranilate Synthase

A master mix containing 100 mM NH4Cl, 10 mM $MgCl_2$, 0.1 mM EDTA, 1 μM of WT or mutant TrpE, 20 μM chorismate, and 20 mM of Tris (pH 9) was made for each reaction to a final volume of 199 μl. Either Trp or 5-flurotryptophan was also added in 1 μl amounts at concentrations ranging from 0.025 to 24 μM. The readings for fluorescence emission (anthranilate) within the range of 480–512 nM were taken using the POLARstar Omega plate reader.

Alamar Blue Assays

In a 96-well plate, bacterial cultures were started at an OD_{600} of 0.003. After 5 days, resazurin reagent was added, and cells were kept in a shaking 37°C incubator for another 1–2 days. Plates were read, and the MIC was determined as the first concentration at which the color changes.

Mouse Pharmacokinetic Study and Sample Preparation

A single dose of 5-FABA, 6-FABA, and the corresponding esters was administered intraperitoneally or orally at 25 mg/kg to female CD-1 mice, 4–6 weeks of age. Blood samples were collected in heparinized tubes at six to eight serial time points between 0 and 24 hr postdosing. Plasma was recovered following centrifugation for 10 min at 1,000 × *g*. Plasma levels of 5-FABA, 6-FABA, and the corresponding esters were quantified by high-pressure liquid chromatography coupled to tandem mass spectrometry (LC-MS/MS) following protein precipitation with a 9:1 acetonitrile-to-plasma ratio, with diclofenac as internal standard. Standards, quality control samples, and blanks in commercial mouse plasma were used.

LC-MS Conditions

The analysis was performed on a Sciex Applied Biosystems API4000 triple-quadrupole mass spectrometer coupled to an Agilent 1260 HPLC system. Sample analysis was accepted if the low-level quality control samples were within ±20% of nominal concentration and ±15% for mid- and high-level quality control samples.

Acetonitrile with 0.1% formic acid was used as extractant. Gradient elution conditions with a Fluophase 2.1 × 100 mm 5 U column were used. The mobile phase A was 0.1% formic acid in deionized water, and mobile phase B was 0.1% formic acid in acetonitrile. The flow rate was 0.6 ml/min.

SUPPLEMENTAL INFORMATION

Supplemental Information includes six figures and four tables and can be found with this article online at http://dx.doi.org/10.1016/j.cell.2013.10.045.

AUTHOR CONTRIBUTIONS

Y.J.Z., E.J.R., V.D., S.M.B., and J.C.S. conceived and designed the experiments. Y.J.Z., A.C.R., B.M.S., M.C.R., S.G., D.W., and A.T. performed the experiments. Y.J.Z., C.H., and T.R.I. built and utilized the tools for genomic analysis of the transposon screen. Y.J.Z. and E.J.R. prepared the manuscript, and T.R.I., J.C.S., V.D., A.C.R., and S.M.B. edited the manuscript.

ACKNOWLEDGMENTS

We thank Michael DeJesus, Chris Sassetti, and Justin Pritchard for their ongoing collaboration and thoughtful conversations about genomic profiling in Mtb. We thank Xiaohua Li and Spandana Valluru for technical support. Noman Sidddiqi and Larry Pipkin manage and run our BL3 facility; we thank them for their support. We thank our tremendous scientific community, including Marcia Goldberg, Laurence Rahme, Sarah Fortune, and Barry Bloom, for its constant support and feedback. The project described was supported by the National Institutes of Health (T32 GM007753 to Y.J.Z., R01 AI 098637 to S.M.B., and P01 AI095208 to J.C.S. and E.J.R.), the Herchel Smith Graduate Fellowship of Harvard and Cambridge University (to Y.J.Z.), and the Wolfe-Welch Chair (to J.C.S.). The content is solely the responsibility of the authors and does not necessarily represent the official views of the National Institutes of Health.

Received: August 21, 2013
Revised: October 11, 2013
Accepted: October 18, 2013
Published: December 5, 2013

REFERENCES

Alberati-Giani, D., Malherbe, P., Ricciardi-Castagnoli, P., Köhler, C., Denis-Donini, S., and Cesura, A.M. (1997). Differential regulation of indoleamine 2,3-dioxygenase expression by nitric oxide and inflammatory mediators in IFN-gamma-activated murine macrophages and microglial cells. J. Immunol. *159*, 419–426.

Baker, T.I., and Crawford, I.P. (1966). Anthranilate synthetase. Partial purification and some kinetic studies on the enzyme from *Escherichia coli*. J. Biol. Chem. *241*, 5577–5584.

Bold, T.D., Banaei, N., Wolf, A.J., and Ernst, J.D. (2011). Suboptimal activation of antigen-specific CD4+ effector cells enables persistence of *M. tuberculosis* in vivo. PLoS Pathog. *7*, e1002063.

Coggins, J.R., Abell, C., Evans, L.B., Frederickson, M., Robinson, D.A., Roszak, A.W., and Lapthorn, A.P. (2003). Experiences with the shikimate-pathway enzymes as targets for rational drug design. Biochem. Soc. Trans. *31*, 548–552.

Cosgrove, D., Gray, D., Dierich, A., Kaufman, J., Lemeur, M., Benoist, C., and Mathis, D. (1991). Mice lacking MHC class II molecules. Cell *66*, 1051–1066.

Desvignes, L., and Ernst, J.D. (2009). Interferon-gamma-responsive nonhematopoietic cells regulate the immune response to *Mycobacterium tuberculosis*. Immunity *31*, 974–985.

Ehrt, S., and Schnappinger, D. (2009). Mycobacterial survival strategies in the phagosome: defence against host stresses. Cell. Microbiol. *11*, 1170–1178.

Ernst, J.D. (2012). The immunological life cycle of tuberculosis. Nat. Rev. Immunol. *12*, 581–591.

Fabri, M., Stenger, S., Shin, D.M., Yuk, J.M., Liu, P.T., Realegeno, S., Lee, H.M., Krutzik, S.R., Schenk, M., Sieling, P.A., et al. (2011). Vitamin D is required for IFN-gamma-mediated antimicrobial activity of human macrophages. Sci. Transl. Med. *3*, 104ra102.

Flynn, J.L. (2006). Lessons from experimental *Mycobacterium tuberculosis* infections. Microbes Infect. *8*, 1179–1188.

Flynn, J.L., Chan, J., Triebold, K.J., Dalton, D.K., Stewart, T.A., and Bloom, B.R. (1993). An essential role for interferon gamma in resistance to *Mycobacterium tuberculosis* infection. J. Exp. Med. *178*, 2249–2254.

Flynn, J.L., Goldstein, M.M., Chan, J., Triebold, K.J., Pfeffer, K., Lowenstein, C.J., Schreiber, R., Mak, T.W., and Bloom, B.R. (1995). Tumor necrosis factor-alpha is required in the protective immune response against *Mycobacterium tuberculosis* in mice. Immunity *2*, 561–572.

Gallegos, A.M., van Heijst, J.W.J., Samstein, M., Su, X., Pamer, E.G., and Glickman, M.S. (2011). A gamma interferon independent mechanism of CD4 T cell mediated control of *M. tuberculosis* infection in vivo. PLoS Pathog. *7*, e1002052.

Goodman, A.L., McNulty, N.P., Zhao, Y., Leip, D., Mitra, R.D., Lozupone, C.A., Knight, R., and Gordon, J.I. (2009). Identifying genetic determinants needed to establish a human gut symbiont in its habitat. Cell Host Microbe *6*, 279–289.

Griffin, J.E., Gawronski, J.D., Dejesus, M.A., Ioerger, T.R., Akerley, B.J., and Sassetti, C.M. (2011). High-resolution phenotypic profiling defines genes essential for mycobacterial growth and cholesterol catabolism. PLoS Pathog. *7*, e1002251.

Grusby, M.J., Johnson, R.S., Papaioannou, V.E., and Glimcher, L.H. (1991). Depletion of CD4+ T cells in major histocompatibility complex class II-deficient mice. Science *253*, 1417–1420.

Hagedorn, M., Rohde, K.H., Russell, D.G., and Soldati, T. (2009). Infection by tubercular mycobacteria is spread by nonlytic ejection from their amoeba hosts. Science *323*, 1729–1733.

Hondalus, M.K., Bardarov, S., Russell, R., Chan, J., Jacobs, W.R., Jr., and Bloom, B.R. (2000). Attenuation of and protection induced by a leucine auxotroph of *Mycobacterium tuberculosis*. Infect. Immun. *68*, 2888–2898.

Hood, M.I., and Skaar, E.P. (2012). Nutritional immunity: transition metals at the pathogen-host interface. Nat. Rev. Microbiol. *10*, 525–537.

Ibana, J.A., Belland, R.J., Zea, A.H., Schust, D.J., Nagamatsu, T., AbdelRahman, Y.M., Tate, D.J., Beatty, W.L., Aiyar, A.A., and Quayle, A.J. (2011). Inhibition of indoleamine 2,3-dioxygenase activity by levo-1-methyl tryptophan blocks gamma interferon-induced *Chlamydia trachomatis* persistence in human epithelial cells. Infect. Immun. *79*, 4425–4437.

Lee, W., VanderVen, B.C., Fahey, R.J., and Russell, D.G. (2013). Intracellular *Mycobacterium tuberculosis* exploits host-derived fatty acids to limit metabolic stress. J. Biol. Chem. *288*, 6788–6800.

Lesic, B., Lépine, F., Déziel, E., Zhang, J., Zhang, Q., Padfield, K., Castonguay, M.H., Milot, S., Stachel, S., Tzika, A.A., et al. (2007). Inhibitors of pathogen intercellular signals as selective anti-infective compounds. PLoS Pathog. *3*, 1229–1239.

Marrero, J., Rhee, K.Y., Schnappinger, D., Pethe, K., and Ehrt, S. (2010). Gluconeogenic carbon flow of tricarboxylic acid cycle intermediates is critical for *Mycobacterium tuberculosis* to establish and maintain infection. Proc. Natl. Acad. Sci. USA *107*, 9819–9824.

McDonough, K.A., Kress, Y., and Bloom, B.R. (1993). Pathogenesis of tuberculosis: interaction of *Mycobacterium tuberculosis* with macrophages. Infect. Immun. *61*, 2763–2773.

McKinney, J.D., Höner zu Bentrup, K., Muñoz-Elías, E.J., Miczak, A., Chen, B., Chan, W.T., Swenson, D., Sacchettini, J.C., Jacobs, W.R., Jr., and Russell, D.G. (2000). Persistence of *Mycobacterium tuberculosis* in macrophages and mice requires the glyoxylate shunt enzyme isocitrate lyase. Nature *406*, 735–738.

Mogues, T., Goodrich, M.E., Ryan, L., LaCourse, R., and North, R.J. (2001). The relative importance of T cell subsets in immunity and immunopathology of airborne *Mycobacterium tuberculosis* infection in mice. J. Exp. Med. *193*, 271–280.

Muñoz-Elías, E.J., and McKinney, J.D. (2005). *Mycobacterium tuberculosis* isocitrate lyases 1 and 2 are jointly required for in vivo growth and virulence. Nat. Med. *11*, 638–644.

Nandi, B., and Behar, S.M. (2011). Regulation of neutrophils by interferon-γ limits lung inflammation during tuberculosis infection. J. Exp. Med. *208*, 2251–2262.

Pandey, A.K., and Sassetti, C.M. (2008). Mycobacterial persistence requires the utilization of host cholesterol. Proc. Natl. Acad. Sci. USA *105*, 4376–4380.

Parish, T. (2003). Starvation survival response of *Mycobacterium tuberculosis*. J. Bacteriol. *185*, 6702–6706.

Pavelka, M.S., Jr., Chen, B., Kelley, C.L., Collins, F.M., and Jacobs Jr, W.R., Jr. (2003). Vaccine efficacy of a lysine auxotroph of *Mycobacterium tuberculosis*. Infect. Immun. *71*, 4190–4192.

Pawlowski, A., Jansson, M., Sköld, M., Rottenberg, M.E., and Källenius, G. (2012). Tuberculosis and HIV co-infection. PLoS Pathog. *8*, e1002464.

Price, C.T., Al-Quadan, T., Santic, M., Rosenshine, I., and Abu Kwaik, Y. (2011). Host proteasomal degradation generates amino acids essential for intracellular bacterial growth. Science *334*, 1553–1557.

Sassetti, C.M., and Rubin, E.J. (2003). Genetic requirements for mycobacterial survival during infection. Proc. Natl. Acad. Sci. USA *100*, 12989–12994.

Scanga, C.A., Mohan, V.P., Yu, K., Joseph, H., Tanaka, K.E., Chan, J., and Flynn, J.L. (2000). Depletion of CD4(+) T cells causes reactivation of murine persistent tuberculosis despite continued expression of interferon gamma and nitric oxide synthase 2. J. Exp. Med. *192*, 347–358.

Selwyn, P.A., Hartel, D., Lewis, V.A., Schoenbaum, E.E., Vermund, S.H., Klein, R.S., Walker, A.T., and Friedland, G.H. (1989). A prospective study of the risk of tuberculosis among intravenous drug users with human immunodeficiency virus infection. N. Engl. J. Med. *320*, 545–550.

Smith, D.A., Parish, T., Stoker, N.G., and Bancroft, G.J. (2001). Characterization of auxotrophic mutants of *Mycobacterium tuberculosis* and their potential as vaccine candidates. Infect. Immun. *69*, 1142–1150.

Subramanian, A., Tamayo, P., Mootha, V.K., Mukherjee, S., Ebert, B.L., Gillette, M.A., Paulovich, A., Pomeroy, S.L., Golub, T.R., Lander, E.S., and Mesirov, J.P. (2005). Gene set enrichment analysis: a knowledge-based approach for interpreting genome-wide expression profiles. Proc. Natl. Acad. Sci. USA *102*, 15545–15550.

Tarshis, M.S., and Weed, W.A., Jr. (1953). Lack of significant in vitro sensitivity of *Mycobacterium tuberculosis* to pyrazinamide on three different solid media. Am. Rev. Tuberc. *67*, 391–395.

Tattoli, I., Sorbara, M.T., Vuckovic, D., Ling, A., Soares, F., Carneiro, L.A., Yang, C., Emili, A., Philpott, D.J., and Girardin, S.E. (2012). Amino acid starvation induced by invasive bacterial pathogens triggers an innate host defense program. Cell Host Microbe *11*, 563–575.

Vandal, O.H., Pierini, L.M., Schnappinger, D., Nathan, C.F., and Ehrt, S. (2008). A membrane protein preserves intrabacterial pH in intraphagosomal *Mycobacterium tuberculosis*. Nat. Med. *14*, 849–854.

van der Wel, N., Hava, D., Houben, D., Fluitsma, D., van Zon, M., Pierson, J., Brenner, M., and Peters, P.J. (2007). *M. tuberculosis* and *M. leprae* translocate from the phagolysosome to the cytosol in myeloid cells. Cell *129*, 1287–1298.

WHO (2007). Protein and Amino Acid Requirements in Human Nutrition (Geneva: WHO Press).

WHO (2011). Global tuberculosis control 2011. http://www.who.int/tb/publications/global_report/2011/en/.

Zelante, T., Fallarino, F., Bistoni, F., Puccetti, P., and Romani, L. (2009). Indoleamine 2,3-dioxygenase in infection: the paradox of an evasive strategy that benefits the host. Microbes Infect. *11*, 133–141.

Zhang, Y., and Mitchison, D. (2003). The curious characteristics of pyrazinamide: a review. Int. J. Tuberc. Lung Dis. *7*, 6–21.

Zhang, Y.J., and Rubin, E.J. (2013). Feast or famine: the host-pathogen battle over amino acids. Cell. Microbiol. *15*, 1079–1087.

Zhang, Y.J., Ioerger, T.R., Huttenhower, C., Long, J.E., Sassetti, C.M., Sacchettini, J.C., and Rubin, E.J. (2012). Global assessment of genomic regions required for growth in *Mycobacterium tuberculosis*. PLoS Pathog. *8*, e1002946.